RESEARCH ARTICLE

Analysis of enamel/restoration interface submitted cariogenic challenge and fluoride release

Raquel Viana Rodrigues[1,2] | Camila Sobral Sampaio[1,3] | Aline Carvalho Girotto[1] | Caroline Paiuta Pinhatti[4] | Alexsandra Shizue Iwamoto[4] | Anderson Zanardi de Freitas[5] | Gláucia Maria Bovi Ambrosano[4] | Regina Maria Puppin-Rontani[4] | Fernanda Miori Pascon[4]

[1]Department of Restorative Dentistry, Piracicaba Dental School, UNICAMP, Piracicaba, Brazil

[2]Department of Oral Health Sciences, UBC Faculty of Dentistry, Vancouver, Canada

[3]Department of Biomaterials, Universidad de Los Andes, Santiago, Chile

[4]Department of Health Sciences and Pediatric Dentistry, Piracicaba Dental School, UNICAMP, Piracicaba, Brazil

[5]Center for Laser and Applications, Nuclear and Energy Research Institute, USP, São Paulo, Brazil

Correspondence
Fernanda Miori Pascon, Department of Health Sciences and Pediatric Dentistry, Pediatric Dentistry Area, Piracicaba Dental School, University of Campinas, P.O. BOX 52, 13414-903, Piracicaba, Brazil.
Email: pascon@unicamp.br

Abstract

The treatment of high-risk patients still is a challenge. The understanding and development non-invasive, non-destructive, and non-ionizing techniques, can help to guide the treatment and the diagnosis of primary and recurrent caries. The present study evaluated the behavior of enamel/restoration interface after a cariogenic challenge by Fourier domain optical coherence tomography (FD-OCT), scanning electron microscopy (SEM) examination, and the fluoride release of the different restorative materials. Cavities (1.5×0.5 mm) were performed in enamel surface and divided into groups ($n = 8$): glass ionomer cement (GIC), resin-modified glass ionomer cement (RMGIC), and resin composite (RC). The samples were submitted to pH-cycling, and the solutions analyzed for cumulative fluoride by ion-analyzer. The morphology was analyzed by SEM through replicas. The optical attenuation coefficient (OAC) was calculated through exponential decay from the images generated by FD-OCT. Data were analyzed considering $\alpha = 0.05$. OAC values increased for all groups after pH-cycling indicating demineralization ($p < .05$). Considering the remineralizing solution, RMGIC presented higher fluoride release rate, followed by GIC, while RC did not release any fluoride. Yet for the demineralizing solution, RMGIC and GIC released similar fluoride rates, overcoming RC ($p < .05$). Micrographs revealed no changes on the restorations margins, although enamel detachment was observed for RC and GIC after pH-cycling.

KEYWORDS
dental enamel, dental materials, enamel demineralization, optical coherence tomography, scanning electron microscopy

1 | INTRODUCTION

As the world dentistry is walking to a digital era, science searches for no invasive diagnostic tools that can be used clinically. Optical coherence tomography (OCT) is a non-invasive, non-destructive, and non-ionizing technique used in vitro and clinically, to create cross-sectional images of whole internal biological structures (Son, Jung, Ko, & Kwon, 2016; Youngquist, Carr, & Davies, 1987). OCT is based on low-coherence interferometry: light is projected over a sample, and the signal intensity of light backscattered by the scattering medium provides information about the depth and density of structures in the sample (Huang et al., 1991).

Therefore, OCT is a no destruct promising technique to diagnose the first stage of caries disease allowing their clinical management and

progression through the longitudinal evaluation of enamel demineralization (Kitasako et al., 2019; Macey et al., 2021). The technique is based in optical laws, where porous created in demineralized tissue increase the light scattering, causing changes on the optical properties of enamel during the decay process and allowing quantitative measurement of optical properties providing a repeatable means of tissue characterization (Jones & Fried, 2006; Kang, Darling, & Fried, 2011). Among these optical properties, the optical attenuation coefficient (OAC) is one of the units of measurement that reflect demineralization and remineralization enamel (Popescu, Sowa, Hewko, & Choo-Smith, 2008), corresponding of how much light is attenuated in the tissue (Sowa, Popescu, Friesen, Hewko, & Choo-Smith, 2011). For instance, higher OAC values are associated to dental demineralization (Baptista et al., 2012; Mandurah et al., 2013; Popescu et al., 2008).

Adding to the dynamic process of enamel demineralization, we have to consider, as well how restorative materials could interact with the enamel, since recurrent caries have been considered the main reason for the restorations replacement (Mjör, 2005). Moreover, the understanding that the restorative treatment does not cure the caries disease and the lesions recurrence on restorations margins result from neglecting to treat caries as a disease before placing a restoration, it is especially critical for high caries risk/activity patients (Rao & Malhotra, 2013; Swarn & Swift, 2012). Part of the caries treatment is encouraging remineralization (Swarn & Swift, 2012) and preventing demineralization of cavity margins and walls (Mickenautsch et al., 2009). Thus, attention has been applied in restorative materials that have fluoride content and the ability to inhibit recurrent caries, which is considered an important clinical property (Vermeersch, Leloup, & Vreven, 2001).

Combining this information and looking to the future, more information about technologies that could collect information and access restorations margins are important and relevant. Consequently, more studies addressing restorative materials using OCT technology still warrant investigation, providing an understand how to control high caries risk/activity patients, to prevent caries lesions formation and to provide more basis for the clinical application of dental materials. The aim of the in vitro study was to evaluate the behavior of enamel/restoration interface after a cariogenic challenge by FD-OCT, scanning electron microscopy (SEM) examination, and the fluoride release of the different restorative materials.

2 | MATERIALS AND METHODS

2.1 | Specimen preparation

Twenty-four bovine incisors free from cracks or structural defect were selected and randomly assigned into three groups ($n = 8$). The number of samples was determined based on a pilot study. Teeth were stored in 0.1% thymol solution until use.

The teeth were pumiced and the roots were cut off at the cement–enamel junction using a double-faced diamond disk (KG Sorensen, Barueri, SP, Brazil). The enamel–buccal surface was ground flat under water using a 400 grit SiC paper. Spherical cavities (1.5 ± 0.3 mm diameter × 0.5 mm depth) were prepared on the buccal surface of each tooth using a diamond bur (#3131, Microdont, São Paulo, SP, Brazil), in a high-speed hand-piece with a water-cooled (Kavo SA, Joinville, SC, Brazil), using a standardized cavity preparation device (Elquip, São Carlos, SP, Brazil), determining the depth of preparation. All cavity margins were established in enamel.

2.2 | Restorative procedure

The teeth were restored according to the materials: Conventional Glass Ionomer Cement (GIC; Ketac Molar Easymix, 3 M ESPE Dental Products, Sumaré, SP, Brazil); Resin-Modified GIC (RMGIC; Vitremer, 3 M ESPE Dental Products, Sumaré, SP, Brazil); and Resin Composite system (RC; AdperTM Single Bond2 + Filtek Z350, 3 M ESPE Dental Products, Sumaré, SP, Brazil), according to manufacturer's recommendations (Table 1). All restorative procedures were performed by the same trained operator. The teeth were stored in 100% humidity at 37°C. After 24 hr, finishing was performed with a diamond bur (#3139 FF; Microdont, São Paulo, SP, Brazil), and polishing by Sof-LexTM system (3 M ESPE Dental Products, Sumaré, SP, Brazil) always water-cooled.

2.3 | Optical coherence tomography analysis

Specimens were positioned in a stander individualized platform to guarantee orientation before and after pH-cycling scans, the sample humidity was controlled by applying water droplets on the surface of the peripheral enamel to the analyzed area. So, the enamel was kept hydrated but there was not water on the reading area. Subsequently specimens were examined using a Fourier Domain (FD-OCT) system with a superluminescent LED at 930 nm with 2 mW power (OCP930SR Thorlabs Inc.). Data acquisition and processing are performed using the integrated software package. This experimental set-up was used to obtain nine images that were 4,000 × 1,500 μm (2,000 × 512 pixels) in size. These images presented the axial resolution of 6.0 μm (in air) and lateral resolution of 6.0 μm. Figure 1 shows illustrative images of restored enamel. It could be observed that in GIC and RMGIC the presence of bubbles and pores due to air incorporation during the manipulation that occurs less frequently in RC because it is a single past material. Moreover, it is possible to see the high reflectance of GIC due to glass particles, a characteristic that did not allow the light go through the sample. The dark area in RMGIC and RC is due to the index of refraction of the monomers that usually are transparent materials.

Software developed in LabView 8 was used to obtain the total OAC for all images. The total OAC was calculated based on the exponential decay of the detected light intensity (backscattered), according to the following equation: $I = I_0 e^{-2 \propto z} + C$; where I represents the detected intensity, I_0 is the intensity value of the source when traveling through the specimen, α is the total optical attenuation coefficient,

TABLE 1 Restorative materials used in the study according to the composition and manipulation details

Material/batch #	Composition	Materials' manipulation details
Conventional glass ionomer cement: Ketac molar Easymix #458691	Powder: Aluminum–calcium–lanthanum–fluorosilicate glass, and 5% polycarbonate acid Liquid: Polycarbonic acid and tartaric acid	The material was proportioned (1:1) on the mixing block. A flexible spatula was used for material agglutination. A homogeneous mixture was obtained. The cavities were pre-treated with a drop of liquid for 10 s, washed with water and dried for 3 s. next, the material was inserted into the cavity using a Centrix syringe (Centrix Inc., Shelton, Connecticut). A polyester matrix strip was positioned over the restoration and the material was compressed with a glass slide. After curing, the material was coated with one layer of petroleum jelly.
Resin-modified glass ionomer cement: Vitremer #1120900643	Powder: Fluoraluminosilicate glass, redox catalyst system, and pigments Liquid: Polycarboxylic acid modified with pedant methacrylate groups, Vitrebond copolymer, water, HEMA, and photoinitiators Primer: Vitrebond copolymer, HEMA, ethanol, and photoinitiators	The primer was applied using a microbrush with slight friction for 30 s, gently air-dried for 15 s and then cured for 40 s. the GIC was manipulated (powder: Liquid ratio 2.5/1 by weight) on a glass plate and inserted into the cavity using a Centrix syringe. A polyester matrix strip was positioned over the restoration and the material was compressed with a glass slide. The glass slide was removed and the material was photocured for 40 s using Bluephase G2 (Ivoclar Vivadent, Barueri, SP, Brazil) with the light intensity of 1,200 mW/cm^2, which was checked every 8 restorations using curing radiometer model 100 (Demetron research Corp, The United States). The glaze was then applied on the restoration surface and cured for 20 s.
Resin composite Filtek Z350: #1202700114	Organic matrix: Bis-GMA, UDMA, TEGDMA, and bis-EMA resins Inorganic particles: The fillers are a combination of non-agglomerated/non-aggregated 20-nm silica filler, non-agglomerated/non-aggregated 4–11 nm zirconia filler, and aggregated zirconia/silica cluster filler (comprised of 20 nm silica and 4–11 nm zirconia particles). The mixture was 72.5% inorganic filler by weight (55.6% by volume) for the translucent shades and 78.5% by weight (63.3% by volume) for all other shades	Enamel surfaces were prepared using 37% phosphoric acid gel (Condac37-FGM, #050112) for 30 s, rinsed for 30 s and dried with oil-free air. Adper single bond 2 was applied in 2 consecutive layers, dried for 5 s, and then light-cured for 10 s. all cavities were restored and photocuring for 20 s using a Bluephase G2 with the light intensity of 1,200 mW/cm^2, which was checked every 8 restorations using curing radiometer model 100.

Abbreviations: Bis-GMA, bisphenol-glycidyl methacrylate; HEMA, 2-hydroxyethyl methacrylate; TEGDMA, triethylene glycol dimethacrylate; UDMA, urethane dimethacrylate.

z is the depth analyzed, and C is a constant used to account for the background noise signal. The OAC of each specimen and each area was derived from the arithmetic mean for all images evaluated, as described by previous studies (de Cara et al., 2012; de Cara, Zezell, Ana, Maldonado, & Freitas, 2014).

Nine images were taken from each specimen through the restoration diameter, before and after pH-cycling, to provide an accurate analysis of the restoration perimeter. The images were evaluated at different regions of interest (ROIs) at two distances from the restoration margin: one at 0–200 μm and another at 200–400 μm (Figure 2). The OAC was calculated from predefined depths of 25–120 μm (Figure 3) for all samples, to avoid the first peak at 20 mm (de Cara et al., 2014).

2.4 | The pH-cycling model

The pH-cycling model was used to simulate a cariogenic challenge. Except for a 1 mm margin around the restoration, the specimens were coated with two layers of acid-resistant varnish (Colorama, São Paulo, SP, Brazil). The specimens were immersed in demineralizing solution (2.0 mmol/L Ca and P, 0.075 mol/L acetate buffer, 0.04 μg F/ml, 2.2 ml/mm^2 of surface enamel, pH 4.7; final solution volume = 21.15 ml) for 6 hr and remineralizing solution (1.5 mmol/L Ca, 0.9 mmol/L P, 0.15 mol/L KCl, 0.02 mol/L Tris buffer, 0.05 μg F/ml, 1.1 ml/mm^2 of surface enamel, pH 7.0; final solution volume = 10.58 ml) for 18 hr, at 37°C, for 5 days. Subsequently, the specimens were immersed in remineralizing solution for an additional
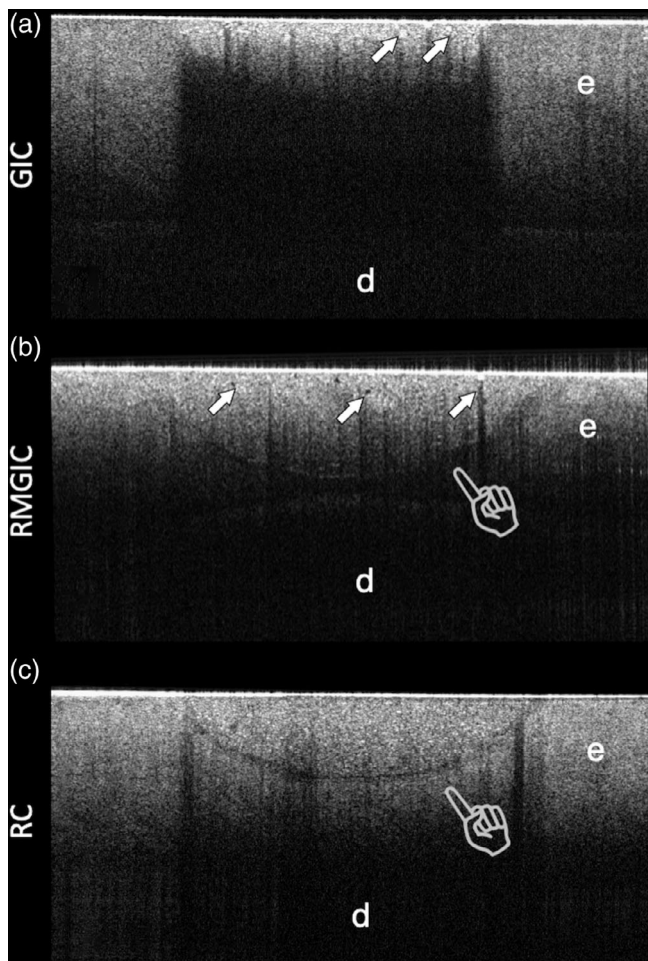
FIGURE 1   Restored enamel with the materials groups. (a) conventional glass ionomer cement (GIC); (b) resin-modified GIC (RMGIC); (c) resin composite (RC); (e) enamel (d) dentin. Arrows indicate the presence of bubbles and pores in a and b. The pointer in b indicates the presence of the primer and in c indicates the presence of the adhesive system applied

48 hr (Rodrigues, Delbem, Pedrini, & Oliveira, 2008). The pH of the solutions was checked in duplicate by the specific electrode (Orion 96-09) and ion-analyzer (Orion EA-940, Orion Research, Boston, Massachusetts) before the specimen's immersion as a standard protocol.

2.5 | Cumulative fluoride release analysis

After the pH-cycling, the total amount of fluoride ions in the demineralizing and remineralizing solutions of each group, was measured in duplicate using the electrode (Orion 96-09) and ion-analyzer (Orion EA-940, Orion Research, Boston, Massachusetts), which had been previously calibrated in triplicate with F standards (0.0625–2 mg F/ml), in TISAB III. The fluoride concentration was expressed as μg F/ml.

2.6 | Scanning electron microscopy analysis

After 24 hr of the restorative procedure, the samples were replicated carried out using heavy and light silicone addition (Express Standard-3 M ESPE, St Paul, Minnesota) and the mold were cast with epoxy resin. Then the samples were subjected to the pH-cycling model. New replicas were made after the pH-cycling. The obtained replicas were fixed on metal stubs with carbon tape and then covered with gold by the metallization process in the Balzers apparatus (SCD 050 sputter coater, Balzers Union Aktiengesellschaft), at 52 mA per 100 s. The samples were analyzed by scanning electron microscopy (SEM; JEOL-JSM-5600 LV, Tokyo, Japan), operating at 15 kV using different magnifications, for the observation of restoration interface and enamel structure surface. For illustration proposes magnification of $\times 40 \pm \times 3$ was selected always keeping the restoration on the center of the image.
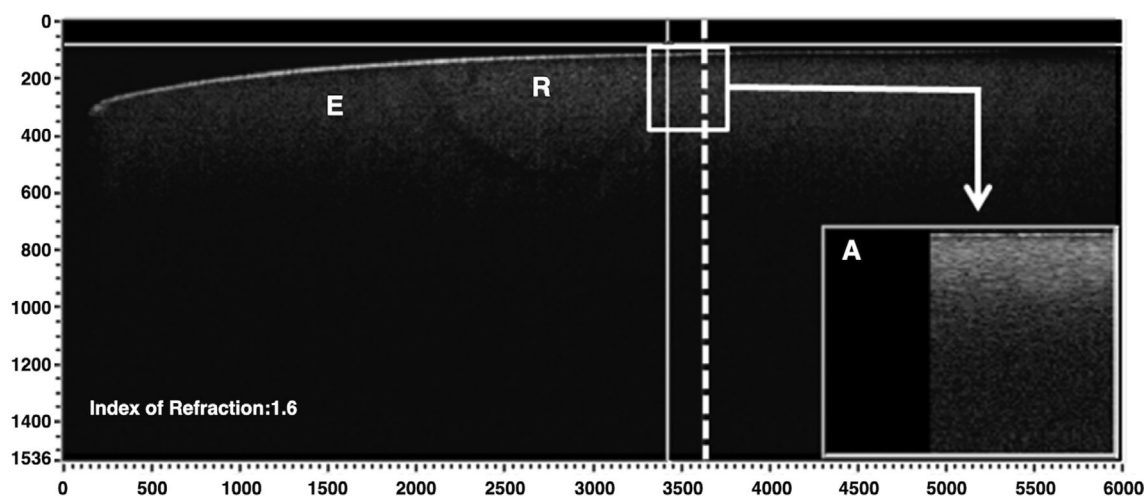

FIGURE 2   Image shows the region of interest (ROI; 0–200 μm) (A) from the restoration margin. The image was obtained from a specimen restored with Resin Composite (RC). (E) Enamel; (R) Restoration. The vertical full and dashed lines defined distance analysis (X-coordinates: Initial position: 3438 μm (full line). End position: 3638 μm (dashed line)
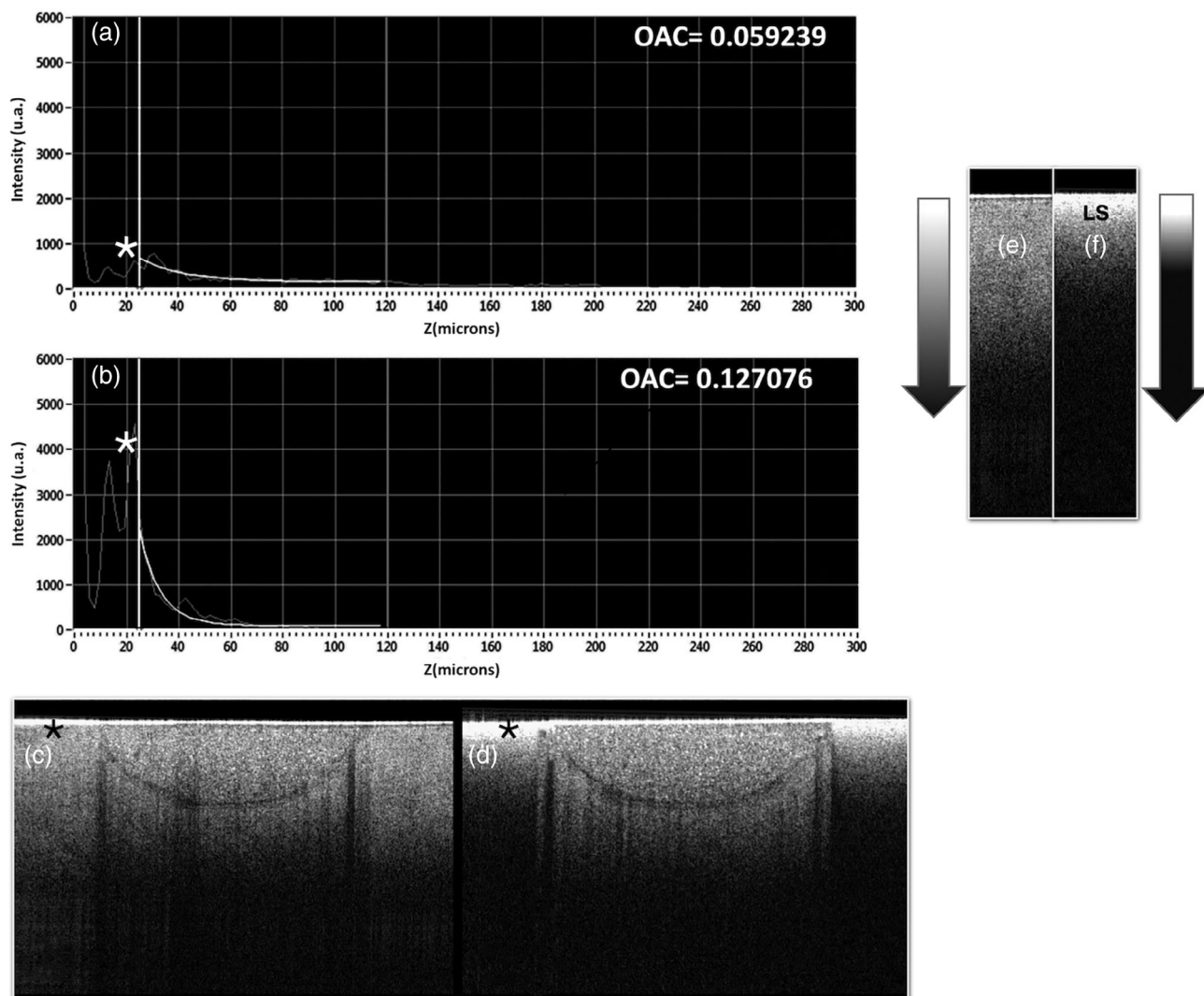
FIGURE 3 Compounded profiles showing OCT signal magnitude (u.a.) related to optical penetration depth. (a) Curve before pH-cycling. (b) Curve after pH-cycling (higher OAC). The depth of each scanned image is delineated by the white and grey vertical lines, representing Z coordinates, located between 25 and 120 μm on the graph. Avoiding the first peak at 20 mm showed by (*) on the graphics and respective images c and d. The part figures e and f exemplify the behavior near the origin, related to the high surface reflectivity of the enamel samples, where it is possible to see the increase in light scattering (LS) of enamel surface after pH-cycling (f). As consequence we observe the increase of OAC through the sample indicate by the arrows

2.7 | Data analysis

2.7.1 | Quantitative analysis

The OAC data were submitted to PROC MIXED procedure for repeated measures. Multiple comparisons were made using the Tukey–Kramer test ($\alpha = 5\%$; SAS Institute Corporation, version 9.1.3; Cary, North Carolina). For the strength of the intra-examiner agreement, 20% of the randomly chosen specimen was examined twice at a weekly interval. The OAC data were analyzed with Intraclass Correlation test and was considered excellent (Intraclass Correlation Coefficient = 0.97; BIOESTAT; version 5.0, 2009). The fluoride release analysis data were submitted to the Anderson-Darling normality test ($\alpha = 5\%$; Minitab Express LLC, 2018). As the data presented normal distribution ($p > .05$), they were submitted one-way ANOVA for each solution and Tukey's test for comparison between groups ($\alpha = 5\%$; Minitab Express LLC, 2018).

2.7.2 | Qualitative analysis

The restoration surface as whole was analyzed, although, the main focus was the enamel/restoration interface to check margins sealing and enamel alteration. It was estipulate the probability to observer the following characteristics: seal margin, gap formation, enamel detachment associated with the restoration margin, and enamel detachment not associated with the restoration margin.

	Region of interest (ROI)			
	0–200 μm		**200–400 μm**	
Material	**Before pH-cycling**	**After pH-cycling**	**Before pH-cycling**	**After pH-cycling**
GIC	0.051 ± 0.0376[*]	0.092 ± 0.0381	0.056 ± 0.0605[*]	0.104 ± 0.0338
RMGIC	0.057 ± 0.0255[*]	0.085 ± 0.0196	0.045 ± 0.0356[*]	0.083 ± 0.0127
RC	0.037 ± 0.0217[*]	0.088 ± 0.0173	0.036 ± 0.0185[*]	0.090 ± 0.0151

TABLE 2 Mean values ± standard deviation of optical attenuation coefficient (OAC) values for materials, before and after pH-cycling and region of interest
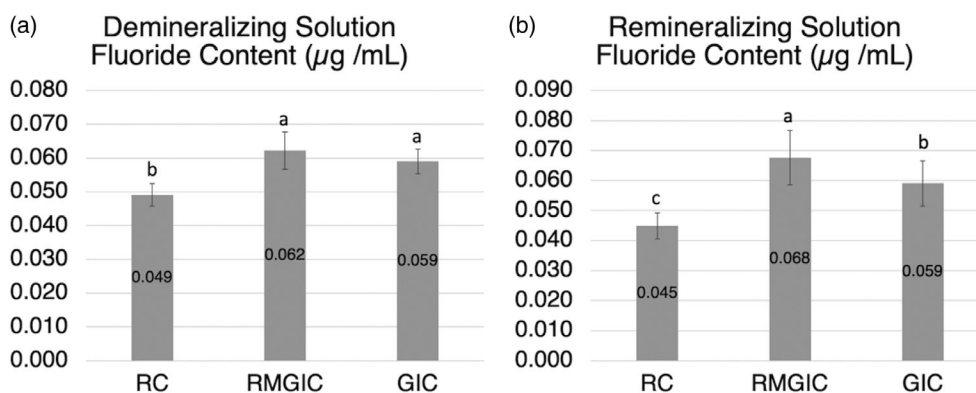
Note: Asterisks (*) indicate statistic difference between before and after pH-cycling of OAC values for the materials (Tukey–Kramer test, $\alpha = 5\%$).

Abbreviations: GIC, conventional glass ionomer cement; RMGIC, resin-modified glass ionomer cement; RC, resin composite.

FIGURE 4 Bars graphic presenting the mean values ± standard deviation of the fluoride release (μg/ml) by the restorative materials after the cariogenic challenge (pH-cycling): demineralizing (a), remineralizing solution (b). Different lowercase letters indicate statistic difference between the materials ($p < .05$). GIC, conventional glass ionomer cement; RMGIC, resin-modified glass ionomer cement; RC, resin composite

3 | RESULTS

3.1 | Optical attenuation coefficient analysis

Table 2 shows OAC values (means and *SD*). Statistical analysis showed no significant interaction between the studied factors (material, pH-cycling, and ROIs; $p = .9740$). Regardless of the material ($p = .3525$) or ROIs ($p = .8509$), a significant difference was found between before and after pH-cycling ($p < .0001$). After pH-cycling it was observed that the OAC values increased (Figure 3).

3.2 | Fluoride release analysis

The restorative materials showed different fluoride release rate ($p < .05$). Higher fluoride release rate was observed in the remineralizing solution for the RMGIC (0.068 ± 0.009), followed by GIC (0.059 ± 0.008), while RC did not release any fluoride. However, for the demineralizing solution, RMGIC (0.062 ± 0.006) and GIC (0.059 ± 0.004) released similar rates, both being superior to RC. RC in both the remineralizing (0.045 ± 0.004) and the demineralizing solutions (0.049 ± 0.003) had a lower rate of fluoride content after cariogenic challenge compared with other materials ($p < .05$), configuring as the no release of fluoride as expected (Figure 4).

3.3 | Scanning electron microscopic analysis

The micrographs reveal no changes on the restorations margins after cariogenic challenge (Figure 5). The enamel surface detachment was observed for RC and GIC materials on some points of enamel surface, however not associated with the restoration margins. The impression material pulling (part of the replica methodology procedure) caused the enamel surface detachment revealing the enamel fragile structure after the cariogenic challenge.

4 | DISCUSSION

The present study evaluate the effect of pH-cycling on restored enamel, analyzing material's cumulative fluoride release, SEM surface examination through replicas, and OAC to investigate demineralization process, which occurs commonly in high-risk caries patients.

During recent years, OCT technology has shown great development. Most of the studies in the dental literature have used polarization-sensitive OCT (PS-OCT; Can, Darling, & Fried, 2008; Chong, Darling, & Fried, 2007; Jones, Darling, Featherstone, & Fried, 2006; Jones & Fried, 2006; Kang et al., 2011). Because it is possible to remove the confounding influence of surface reflections and native birefringence to enhance the resolution of the surface of caries
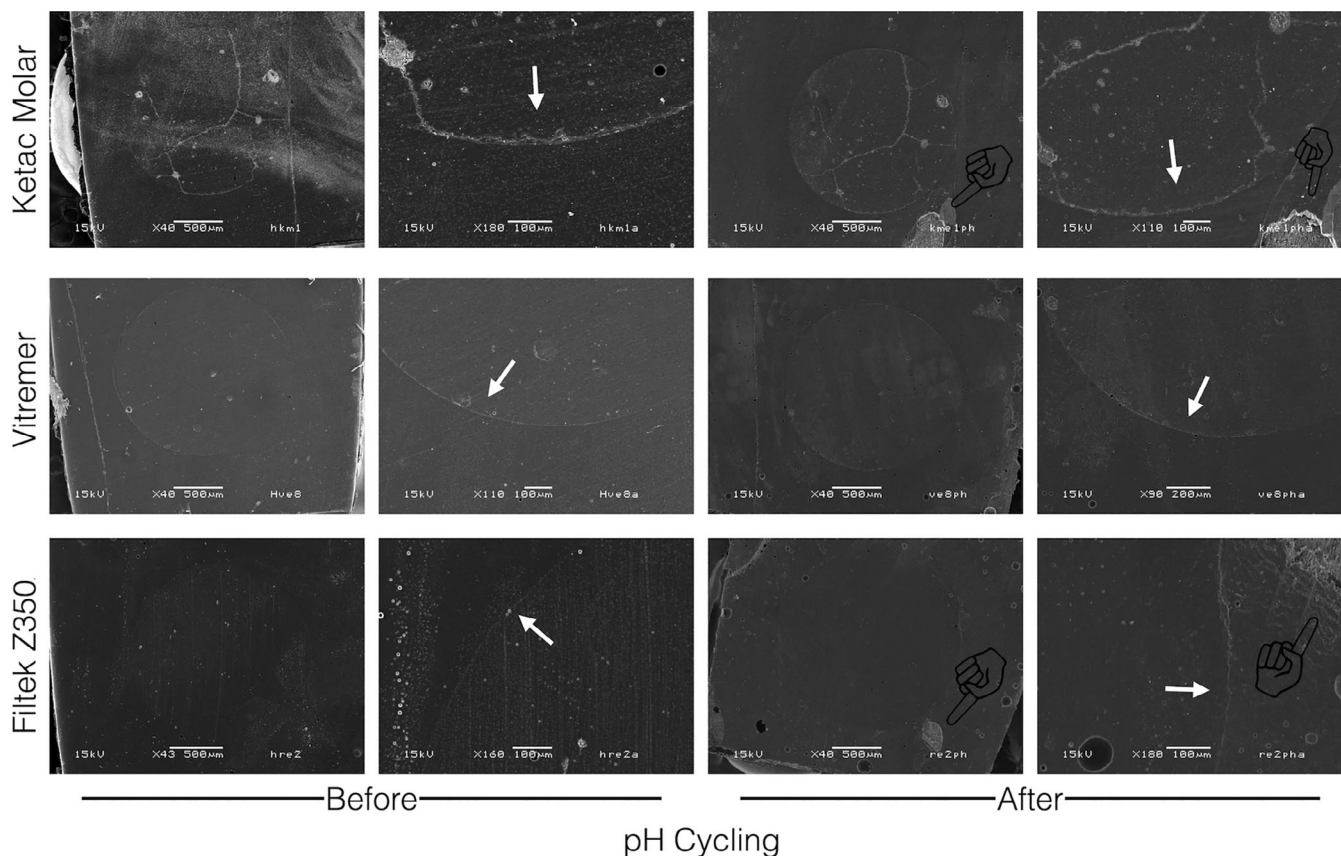
FIGURE 5 Representative scanning electron micrographs of the restorations replicas. Initial magnification of ≅×40 followed by zoom magnifications to analysis specific margins areas. The micrographs before and after the pH-cycling presented seal margins showed by the white arrow. Peripheric enamel surface detachment (black pointers) is observed for RC and GIC materials caused by the impression material pulling after pH-cycling

lesion structure. However, FD-OCT improved signal-to-noise ratio and scanning speed (Choma, Sarunic, Yang, & Izatt, 2003). The potential of non-polarization sensitive OCT systems has been underestimated. Studies using conventional OCT without polarization sensitivity have shown successful images and analysis (de Cara et al., 2012, 2014; Freitas et al., 2009; Hariri, Sadr, Shimada, Tagami, & Sumi, 2012; Mandurah et al., 2013; Natsume et al., 2011; Sampaio et al., 2016), giving to the present study confidence and reliability. Also, as part of discerning methodology we used a Software developed in LabView 8 to select the analysis area out of surface reflections, considering the range of depths from 25 to 120 mm, to avoid the first peak at 20 mm (Figures 2 and 3a,b; de Cara et al., 2014). So, standard areas of analyses for numerical quantitative analyses in artificial lesions were established. Taking as parameter what was observed in literature (de Cara et al., 2012, 2014), the optical attenuation had not shown significant variation for depths after 120 mm. For example, Figure 3c showed a scattering region up to the depth of 120 μm from the surface (Damodaran, Rao, & Vasa, 2016). So, 120 μm maximum depth was also assumed in the present study to define the ROIs (Figure 2), keeping the sample orientation, essential parameter, for optical properties such as absorption and scattering distribution; based on the position of their components relative to the irradiating light source (Hariri et al., 2012).

Looking to the presented results the pH-cycling affected the OAC of restored bovine enamel, but no differences were found related to the materials and the ROIs. The pH-cycling exposed the enamel to a challenge simulating a high risk patient oral environment (Rodrigues et al., 2008; Swarn & Swift, 2012). Consequently, creating an characteristic in vitro lesions, observed in our study, with well-defined surface zone with an absence of thickness increase and with the formation of another layer of highly reflective apatite mineral (Figure 3c,d; Kang et al., 2011). The lesion reflect the loss of mineral content due partially dissolved crystals, forming porous in enamel. When the light go through porous enamel tissue scatters in multiple directions decreasing the sample signal that is detect by the OCT. Being the OAC the unit that quantifies the diminished signal (Figure 3; Baptista et al., 2012; de Cara et al., 2012, 2014; Mandurah et al., 2013; Popescu et al., 2008). Therefore, we understand that the materials were not able to prevent the formation of intercrystalline spaces and the disorganization of the enamel prismatic structures leading to the enlarge light scattering on the surface (Figure 2; Chong et al., 2007; de Cara et al., 2014; Jones & Fried, 2006; Popescu et al., 2008), and cause stronger optical attenuation at demineralized samples (Table 2; de Cara et al., 2012, 2014).

Although the OAC was statistically similar for all groups before and after pH-cycling we speculate that the internal lesion have

different levels of dissolution, because the observation of the SEM analyses showing detachment for GIC and RC while the integrity of RMGIC enamel was kept (Figure 5). Although, it is a fact that RMGIC showed a higher fluoride release in the remineralizing solution (Figure 4), we cannot affirm that the fluoride release was the factor preventing the enamel detachment for this group. GICs were documented as a potential restorative material for caries prevention (Salas, Guglielmi, Raggio, & Mendes, 2011). Two different mechanisms have been proposed to explain the release of fluoride by these materials into an aqueous environment. The first release mechanism is part of the setting reaction. This mechanism provokes high fluoride release from the GIC over the first 24 hr, due to the reaction between the polyalkenoate acid and the glass particles (Vermeersch et al., 2001). The second one occurs more gradually and results in the constant diffusion of ions through the bulk cement, which occurs when the glass is dissolved in the acidified water of the hydrogel matrix (Vermeersch et al., 2001). Water diffusion into the material is necessary for this setting reaction as well as any fluoride release. Ionomeric materials are more permeable to water, which would be expected to enhance fluoride diffusion and release (Asmussen & Peutzfeldt, 2002). Although in the present study, the restored enamel was immersed into the solutions after 24 hr of the restoration placement, due the finishing procedure performed in the next day, which contained setting reaction release just to the internal restoration walls, forbidding the initial release to the media. Allowing, further, only the second mechanism of fluoride release through gradual water diffusion, and consequently delivering a lower fluoride content amount compare to the setting reaction mechanism (Asmussen & Peutzfeldt, 2002; Vermeersch et al., 2001).

Fluoride release and uptake characteristics depend on the matrices, fillers, and fluoride content, as well as, on the setting mechanisms and environmental conditions of the restorations (Mjör, 2005; Vermeersch et al., 2001). Relying on the literature reported information can help us to understand the lack of statistical difference on restored enamel after pH-cycling in the present study. OCT has been able to detect the mineral loss, but maybe the difference on the mineral content did not change the crystalline morphology, providing no significant changes on OAC. As supported by recent literature, having a resemblance with our results where attenuation coefficient OCT data showed a flow resin composite and a GIC sealants presented similar values after demineralization simulation in vitro (Ei et al., 2018). As well the higher fluoride release of GIC was not enough to generate significant changes on attenuation coefficient compared with the resin composite sealant that did not contained fluoride at all (Ei et al., 2018). Same situation observed on OAC values after pH-cycling, regardless the ROIs from the restored margin, where no differences were found between them (0–200 μm and 200–400 μm) neither among restorative materials groups with respect to mineral loss after cariogenic challenge (Table 2).

These distances were determined based on study using microhardness analysis tool, which observed that the preventive effect of GIC and RMGIC was in that range, 0–400 μm from the restoration margin (Salas et al., 2011). On the other hand, this evidence is not conclusive, since Ayres et al. (2015) found that the use of restorative materials containing fluoride were not able to prevent enamel demineralization affecting the microhardness after pH-cycling, independent of the restoration margin distance. Also, in agreement with the present study, Nee et al. (2014) in a clinical study did not found difference in the lesion depth between the groups with the fluoride-releasing GIC and conventional RC. The authors suggested that a fluoride recharge protocol might help to increase the remineralization especially for GIC (Ayres et al., 2015; Nee et al., 2014). Indicating that in a multifactorial environment, when more factors act simultaneously, only the use of fluoride realize materials could not represent a successful preventive strategy.

While some authors consider in a clinical aspect that prevention of recurrent lesions by the use of fluoride-releasing restorative materials is not satisfying (Mjör, 2005). Current literature suggests that the restorative material might influence the development of secondary caries. However, it should be emphasized that patient-related factors, as the simulation high risk caries challenge by pH-cycling, remain the most important determinant of secondary caries (Nedeljkovic, Teughels, De Munck, Van Meerbeek, & Van Landuyt, 2015), corroborating with our findings. Where even with the detected demineralization (Table 2) and for some groups enamel detachment (Figure 5), indicated by the pointer, all margins were sealed as presented by SEM images (Figure 5), independently of the material.

Facing challenging patient's outcomes and knowing the difficulties to diagnose enamel demineralization is the first stage of caries disease, OCT seems to be a reliable tool since used to evaluate mineral loss (Can et al., 2008; Freitas et al., 2009), assess carious lesion depth and severity, determine the efficacy of chemical intervention, test anti-caries agents (Chong et al., 2007; Jones & Fried, 2006; Kang et al., 2011), and to measure the demineralization in enamel (Chong et al., 2007; Freitas et al., 2009; Jones et al., 2006; Jones & Fried, 2006). OCT has clinical credibility of being a promising applications in a clinical detection and monitoring of early enamel caries (Jones et al., 2006; Kitasako et al., 2019). Moreover, OCT is expected to be a valuable tool for dentists and patients, providing non-invasive and real time diagnostic information related to dental lesions and gaps in the context of operative and preventive treatments (Macey et al., 2021; Natsume et al., 2011; Sampaio et al., 2016). FD-OCT could detect small enamel remineralization changes and there was a significant correlation between optical and mechanical findings (de Cara et al., 2012, 2014). According to the literature, OCT is a reliable technique considering the assessment of patients with caries and/or caries history (Chan et al., 2016; Kitasako et al., 2019; Lenton et al., 2012; Macey et al., 2021; Schneider et al., 2017), where it is need to establish conditions that encourage the remineralization of incipient carious lesions rather than the restorative treatments (Rao & Malhotra, 2013). Reaffirming the need of a digital system can be used non-destructively to measure the demineralization process on smooth enamel surfaces around restorations as showed in this in vitro study, through OAC values. For future in vitro studies, we suggest the combination of EDX analysis to reveal the mineral content to complement the enamel crystalline structure analysis as OCT.

5 | CONCLUSION

The cariogenic challenge affected the bovine enamel margin, causing demineralization showed by the increase of OAC, regardless of the material's fluoride release. RMGIC showed the higher fluoride release rate in the storage solutions. Micrographs revealed no changes on the restorations margins, although enamel detachment was observed for RC and GIC after pH-cycling.

CONFLICT OF INTEREST

The authors declare no conflicts of interest.

DATA AVAILABILITY STATEMENT

Research data are not shared.

ETHICS STATEMENT

This research was conducted respecting the rules of the local Ethical and Research Committee and the policies of the University. No human subjects or identifiable human material was used in this research.

ORCID

Fernanda Miori Pascon https://orcid.org/0000-0003-3337-3121

REFERENCES

Asmussen, E., & Peutzfeldt, A. (2002). Long-term fluoride release from a glass ionomer cement, a compomer, and from experimental resin composites. *Acta Odontologica Scandinavica*, 60(2), 93–97. https://doi.org/10.1080/000163502753509482

Ayres, A. P. A., Tabchoury, C. P. M., Giannini, M., Berger, S. B., Yamauti, M., & Ambrosano, G. M. B. (2015). Effect of fluoride-containing restorative materials on dentin adhesion and demineralization of hard tissues adjacent to restorations. *Journal of Adhesive Dentistry*, 17(4), 337–345. https://doi.org/10.3290/j.jad.a34555

Baptista, A., Kato, I. T., Prates, R. A., Suzuki, L. C., Raele, M. P., Freitas, A. Z., & Ribeiro, M. S. (2012). Antimicrobial photodynamic therapy as a strategy to arrest enamel demineralization: A short-term study on incipient caries in a rat model. *Photochemistry and Photobiology*, 88(3), 584–589. https://doi.org/10.1111/j.1751-1097.2011.01059.x

Can, A. M., Darling, C. L., & Fried, D. (2008). High-resolution PS-OCT of enamel remineralization. *Proceedings of Spie–International Society for Optical Engineering*, 6843, 68430T1–68430T7. https://doi.org/10.1117/12.778787

Chan, K. H., Tom, H., Lee, R. C., Kang, H., Simon, J. C., Staninec, M., ... Fried, D. (2016). Clinical monitoring of smooth surface enamel lesions using CP-OCT during nonsurgical ntervention. *Lasers in Surgery and Medicine*, 48(10), 915–923. https://doi.org/10.1002/lsm.22500

Choma, M., Sarunic, M., Yang, C., & Izatt, J. (2003). Sensitivity advantage of swept source and Fourier domain optical coherence tomography. *Optics Express*, 11(18), 2183–2189. https://doi.org/10.1364/oe.11.002183

Chong, S. L., Darling, C. L., & Fried, D. (2007). Nondestructive measurement of the inhibition of demineralization on smooth surfaces using polarization-sensitive optical coherence tomography. *Lasers in Surgery and Medicine*, 39(5), 422–427. https://doi.org/10.1002/lsm.20506

Damodaran, V., Rao, S. R., & Vasa, N. J. (2016). Optical coherence tomography based imaging of dental demineralisation and cavity restoration in 840 nm and 1310 nm wavelength regions. *Optics and Lasers in Engineering*, 83, 59–65. https://doi.org/10.1016/j.optlaseng.2016.03.005

de Cara, A. C. B., Zezell, D. M., Ana, P. A., Deana, A. M., Amaral, M. M., Vieira, N. D., & de Freitas, A. Z. (2012). Comparative analysis of optical coherence tomography signal and microhardness for demineralization evaluation of human tooth enamel. In J. Popp, W. Drexler, V. V. Tuchin, & D. L. Matthews (Eds.), *Biophotonics: Photonic solutions for better health care III* (Vol. 8427). Belgium: SPIE Photonics Europe. https://doi.org/10.1117/12.922637

de Cara, A. C. B., Zezell, D. M., Ana, P. A., Maldonado, E. P., & Freitas, A. Z. (2014). Evaluation of two quantitative analysis methods of optical coherence tomography for detection of enamel demineralization and comparison with microhardness. *Lasers in Surgery and Medicine*, 46(9), 666–671. https://doi.org/10.1002/lsm.22292

Ei, T. Z., Shimada, Y., Nakashima, S., Romero, M. J. R. H., Sumi, Y., & Tagami, J. (2018). Comparison of resin-based and glass ionomer sealants with regard to fluoride-release and anti-demineralization efficacy on adjacent unsealed enamel. *Dental Materials Journal*, 37(1), 104–112. https://doi.org/10.4012/dmj.2016-407

Freitas, A. Z., Zezell, D. M., Mayer, M. P. A., Ribeiro, A. C., Gomes, A. S. L., & Vieira, N. D. (2009). Determination of dental decay rates with optical coherence tomography. *Laser Physics Letters*, 6(12), 896–900. https://doi.org/10.1002/lapl.200910092

Hariri, I., Sadr, A., Shimada, Y., Tagami, J., & Sumi, Y. (2012). Effects of structural orientation of enamel and dentine on light attenuation and local refractive index: An optical coherence tomography study. *Journal of Dentistry*, 40(5), 387–396. https://doi.org/10.1016/j.jdent.2012.01.017

Huang, D., Swanson, E. A., Lin, C. P., Schuman, J. S., Stinson, W. G., Chang, W., ... Fujimoto, J. G. (1991). Optical coherence tomography. *Science*, 254(5035), 1–4. https://doi.org/10.1002/ccd.23385

Jones, R. S., Darling, C. L., Featherstone, J. D. B., & Fried, D. (2006). Imaging artificial caries on the occlusal surfaces with polarization-sensitive optical coherence tomography. *Caries Research*, 40(2), 81–89. https://doi.org/10.1159/000091052

Jones, R. S., & Fried, D. (2006). Remineralization of enamel caries can decrease optical reflectivity. *Journal of Dental Research*, 85(9), 804–808. https://doi.org/10.1177/154405910608500905

Kang, H., Darling, C. L., & Fried, D. (2011). Repair of artificial lesions using an acidic remineralization model monitored with cross-polarization optical coherence tomography. In *Lasers in Dentistry XVII*, 7884, 78840Q. San Francisco, California, United States. https://doi.org/10.1117/12.878889

Kitasako, Y., Sadr, A., Shimada, Y., Ikeda, M., Sumi, Y., & Tagami, J. (2019). Remineralization capacity of carious and non-carious white spot lesions: Clinical evaluation using ICDAS and SS-OCT. *Clinical Oral Investigations*, 23(2), 863–872. https://doi.org/10.1007/s00784-018-2503-1

Lenton, P., Rudney, J., Chen, R., Fok, A., Aparicio, C., & Jones, R. S. (2012). Imaging in vivo secondary caries and ex vivo dental biofilms using cross-polarization optical coherence tomography. *Dental Materials*, 28(7), 792–800. https://doi.org/10.1016/j.dental.2012.04.004

Macey, R., Walsh, T., Riley, P., Hogan, R., Glenny, A.-M., Worthington, H., ... Ricketts, D. (2021). Transillumination and optical coherence tomography for the detection and diagnosis of enamel caries. *Cochrane*

Database of Systematic Reviews, *1*, 4734. https://doi.org/10.1002/14651858.CD013855

Mandurah, M. M., Bakhsh, T. A., Tagami, J., Sadr, A., Shimada, Y., Kitasako, Y., ... Sumi, Y. (2013). Monitoring remineralization of enamel subsurface lesions by optical coherence tomography. *Journal of Biomedical Optics*, *18*(4), 046006. https://doi.org/10.1117/1.JBO.18.4.046006

Mickenautsch, S., Yengopal, V., Leal, S. C., Oliveira, L. B., Bezerra, A. C., & Bönecker, M. (2009). Absence of carious lesions at margins of glass-ionomer and amalgam restorations: A meta-analysis. *European Journal of Paediatric Dentistry*, *10*(1), 41–46.

Mjör, I. A. (2005). Clinical diagnosis of recurrent caries. *Journal of the American Dental Association*, *136*(10), 1426–1433. https://doi.org/10.14219/jada.archive.2005.0057

Natsume, Y., Nakashima, S., Sadr, A., Shimada, Y., Tagami, J., & Sumi, Y. (2011). Estimation of lesion progress in artificial root caries by swept source optical coherence tomography in comparison to transverse microradiography. *Journal of Biomedical Optics*, *16*(7), 071408. https://doi.org/10.1117/1.3600448

Nedeljkovic, I., Teughels, W., De Munck, J., Van Meerbeek, B., & Van Landuyt, K. L. (2015). Is secondary caries with composites a material-based problem? *Dental Materials*, *31*(11), e247–e277. https://doi.org/10.1016/j.dental.2015.09.001

Nee, A., Chan, K., Kang, H., Staninec, M., Darling, C. L., & Fried, D. (2014). Longitudinal monitoring of demineralization peripheral to orthodontic brackets using cross polarization optical coherence tomography. *Journal of Dentistry*, *42*(5), 547–555. https://doi.org/10.1016/j.jdent.2014.02.011

Popescu, D. P., Sowa, M. G., Hewko, M. D., & Choo-Smith, L.-P. (2008). Assessment of early demineralization in teeth using the signal attenuation in optical coherence tomography images. *Journal of Biomedical Optics*, *13*(5), 054053. https://doi.org/10.1117/1.2992129

Rao, A., & Malhotra, N. (2013). The role of Remineralizing agents in dentistry: A review. *Compendium of Continuing Education in Dentistry*, *32*, 25–34.

Rodrigues, E., Delbem, A. C. B., Pedrini, D., & Oliveira, M. S. R. (2008). pH-cycling model to Verify the efficacy of fluoride-releasing materials in enamel demineralization. *Operative Dentistry*, *33*(6), 658–665. https://doi.org/10.2341/08-1

Salas, C. F. C., Guglielmi, C. A. B., Raggio, D. P., & Mendes, F. M. (2011). Mineral loss on adjacent enamel glass ionomer cements restorations after cariogenic and erosive challenges. *Archives of Oral Biology*, *56*(10), 1014–1019. https://doi.org/10.1016/j.archoralbio.2011.03.005

Sampaio, C. S., Rodrigues, R. V., Souza-Junior, E. J., Freitas, A. Z., Ambrosano, G. M. B., Pascon, F. M., & Puppin-Rontani, R. M. (2016). Effect of restorative system and thermal cycling on the tooth-restoration interface-oct evaluation. *Operative Dentistry*, *41*(2), 162–170. https://doi.org/10.2341/14-344-L

Schneider, H., Park, K., Häfer, M., Rüger, C., Schmalz, G., Krause, F., ... Haak, R. (2017). Dental applications of optical coherence tomography (OCT) in cariology. *Applied Sciences*, *7*, 472. https://doi.org/10.3390/app7050472

Son, S.-A., Jung, K.-H., Ko, C.-C., & Kwon, Y. H. (2016). Spectral characteristics of caries-related autofluorescence spectra and their use for diagnosis of caries stage. *Journal of Biomedical Optics*, *21*(1), 015001. https://doi.org/10.1117/1.jbo.21.1.015001

Sowa, M. G., Popescu, D. P., Friesen, J. R., Hewko, M. D., & Choo-Smith, L. P. (2011). A comparison of methods using optical coherence tomography to detect demineralized regions in teeth. *Journal of Biophotonics*, *4*, 814–823. https://doi.org/10.1002/jbio.201100014

Swarn, A., & Swift, E. J. (2012). Management of high caries risk patients: Part 1-risk assessment. *Journal of Esthetic and Restorative Dentistry*, *24*(4), 233–235. https://doi.org/10.1111/j.1708-8240.2012.00523.x

Vermeersch, G., Leloup, G., & Vreven, J. (2001). Fluoride release from glass-ionomer cements, compomers and resin composites. *Journal of Oral Rehabilitation*, *28*(1), 26–32. https://doi.org/10.1046/j.1365-2842.2001.00635.x

Youngquist, R. C., Carr, S., & Davies, D. E. N. (1987). Optical coherence-domain reflectometry: A new optical evaluation technique. *Optics Letters*, *12*(3), 158–160. https://doi.org/10.1364/ol.12.000158